JOURNAL OF MATERIALS SCIENCE **37** (2002) 1189–1195

Oxygen impurity in self-propagating high-temperature synthesis of NiAl

A. BISWAS, S. K. ROY, J. B. SINGH, MADANGOPAL, K.
Materials Science Division, Bhabha Atomic Research Centre, Mumbai 400085, India
E-mail: abiswas@apsara.barc.ernet.in

N. PRABHU
Department of Metallurgical Engineering and Materials Science, Indian Institute of Technology, Powai, Mumbai 400076, India

The technique of Self-propagating High-temperature Synthesis (SHS) was used to prepare NiAl from compacts using elemental powder mixtures in stoichiometric amounts under vacuum and argon atmosphere. Considerable changes in the oxygen contents of the specimen before and after the SH-synthesis were not observed. But, unusual occurrence of an impurity phase was noticed in the product as second phase precipitate. The sparsely distributed precipitates could be detected only in the Transmission Electron Microscope and was characterized to be an oxide of aluminium (α-Al_2O_3) containing nickel oxide (NiO), whose solubility in α-Al_2O_3 at room temperature has not been reported earlier. The occurrence of this phase could be traced to the oxygen on the surface of the reactant particles.

1. Introduction

Self-propagating High temperature Synthesis (SHS) or Combustion Synthesis is a novel method of preparing advanced materials using the exothermic reaction which was discovered by Merzhanov *et al*. [1] in 1967. Chemical reactions that are sufficiently exothermic can transform the mixture of the reactants spontaneously into products when initiated and propagate through the reactants' mixture in the form of a combustion wave and this is the basis of Self-propagating High temperature Synthesis (SHS) or Combustion Synthesis process [2]. The final product is obtained progressively without requiring any additional heat. Two variants of this process are recognized, namely plane wave propagation (PWP) mode and the thermal explosion (TE) mode. The plane wave propagation mode involves initiating the reaction by triggering or rapid heating of one end of the specimen and is driven by the exothermicity of the reaction. In the thermal explosion mode, the compacted reactant powders are heated up at a sufficiently high constant rate until the ignition temperature is reached when the reaction is initiated uniformly throughout the sample. Various aspects of this process have been reviewed in great technical details by Munir and Anselmi-Tamburini [3], Moore and Feng [4] and more recently by Verma *et al*. [5]. SHS is both efficient and attractive for the preparation of intermetallics like NiAl because it utilizes its high heat of formation (118.4 kJ/mole) [6] and apart from providing improved purity of the product it assures the exactness of the product chemistry which is very crucial but extremely difficult to achieve by other conventional techniques. Besides, this is even more relevant in the case of NiAl because of the fact that the tensile ductility of the polycrystalline NiAl which is unacceptably poor, can be significantly improved by keeping the composition very close to the stoichiometry and purity of the alloy very high [7].

One of the major advantages of this technique is the high reaction temperature that results in higher purity of the products by volatilizing low boiling point impurities. This effect of self-purification during SHS is discovered by Martirosayn *et al*. [8]. Merzhanov [9], in a recent article has reviewed the studies of systematic analysis of self-purification phenomena in the elemental systems by a number of Russian scientists. They found reduction in the amount of the following impurities after combustion: H_2, O_2, S, Na, K, Ca, Mg etc. Crider [10] too mentioned about this purification effect and also noted the possibility of removal of oxide films from the surfaces of metal particles by a reduction process. Holt and Munir [11] have carried out spectrochemical analysis and shown a significant decrease in the level of impurities as a result of combustion in Ti-C system. Chang *et al*. [12] have shown that much of the impurities namely aluminium, calcium, iron and silicon, are removed during the combustion synthesis of TiC which illustrates the self-purifying effect of SHS due to the high temperature generated by the reaction. Kecskes *et al*. [13], however, have alerted that the self-purifying nature of SHS gets limited if the powders contain non-volatile contaminants and significant amounts of these impurities (like iron in Ti-B and Ti-C systems) may remain in the product. Moreover, SHS is likely to remove the surface oxygen of aluminium particles as they are capable of forming volatile suboxides in case of combustion of aluminide system. Bloshenko *et al*. [14]

have discussed in detail the process of self-purification of SHS products of oxygen impurities for both the following cases: (1). where impurity oxygen is present in the form of an oxide film around the initial powders (Mo + 2Si and Mo + B systems) and (2). where oxygen is in solid solution in Ti particles (Ti + C system). Although the above-mentioned advantages are well accepted in the literature, in some cases it may not be completely unlikely to encounter impurity phases in the combustion synthesized products even when the chemical composition of the product does not change much and remains well within the acceptable range of the intended stoichiometry. In the present paper, the role of oxygen impurity of metallic particles of 3N purity during synthesis of NiAl from elemental powder mixtures in thermal explosion mode of SHS is reported. The current work presents possibly the first ever report of the occurrence of this phase during SHS in Ni-Al system.

2. Experimental procedure

All the experiments were carried out both under vacuum (10^{-5} mbar) and in argon atmosphere with high purity Ni (99.9%) and Al (99.9%) powders, mixed thoroughly in a tumbler ball mill to the stiochiometry corresponding to B2 NiAl (50 : 50) compound and cold pressed in a single-acting hydraulic press into cylindrical specimens of 12 mm diameter and 6–8 mm height. No liquid medium was used during mixing. The compaction pressure was varied from 75 MPa to 150 MPa and the resultant variation in initial green density was from 55% to 65% of theoretical. Three different particle sizes of nickel and one particle size of aluminium were used. The details of the raw materials are given in Table I. The reactions were carried out by SHS technique in thermal explosion mode. The specimen, in which a thin 200 μm diameter B-type (Pt-6Rh/Pt-30Rh) thermocouple was embedded, was put into the cold furnace and the furnace was started with a pre-programmed linear heating rate which varied between 5° C/min to 60° C/min. The output from the thermocouple was collected online a on strip-chart recorder. The microstructural characterization of the product was carried out by optical microscope, SEM and TEM. X-ray diffraction (XRD) was done for phase analysis. EPMA was used for bulk chemical analysis. The etchant used for optical microscopy and SEM had the following composition: conc. HNO_3 - 1 part, H_2O - 2 parts. Specimens for TEM were prepared by cutting 3 mm diameter disc from 200 μm thick slices of the synthesized product followed by dimpling and ion-milling. Ion-milled samples were subsequently jet-thinned to get rid of the ion-damaged areas. Specimens were made from the products of all the three different nickel particle sizes. Electron diffraction was carried out in a JEOL 2000 FX transmission electron microscope. Composition analyses of the precipitates observed in TEM specimens were carried out in a 200 kV Analytical Transmission Electron Microscope (CM 200, Philips) by using the Energy Dispersive X-ray Spectroscopy (EDAX system). No other spectroscopic techniques of better accuracy like EPMA could be used because of the small size of the precipitates. Oxygen analysis of all the reactant powders and the product were carried out by inert gas fusion method.

TABLE I Properties of the initial reactant powders

Powder		Nickel		Aluminium
Symbol	Ni 1	Ni 2	Ni 3	Al
Purity (%)	99.9	99.9	99.9	99.9
Size (d_{50})	10.94 μm	110.83 μm	129.57 μm	41.94 μm
Nature	Agglomerate	Agglomerate	Agglomerate	Atomized
Source	Aldrich	Indigenous	Indigenous	ALCOA

3. Results

3.1. Thermal explosion

A typical time-temperature profile of a powder compact containing Ni 1 powder during thermal explosion is shown in Fig. 1. The combustion behaviour has been found to depend on the particle size of nickel. During all the rates of heating, the compacts containing Ni 1 behaved similarly and the combustion temperature always exceeded the melting temperature of NiAl. The coarse nickel powders result in low combustion temperature and incomplete conversion at lower rates of heating. However, beyond a threshold rate of heating namely 35° C/min, the combustion temperature is found to exceed the melting point of the product for all the three varieties of nickel powders (Ni 1, Ni 2 & Ni 3) essentially signifying total conversion.

3.2. Microstructure

The products show dendritic microstructures as the combustion temperature is more than the melting point of the product. Dendrites are found to be much finer in the case of products from Ni 1 which is fine nickel powder. No second phase precipitates are detected in optical microscope or SEM. Fig. 2 displays the typical microstructure of the combustion synthesized product. XRD result shows that the products are (Fig. 3) single-phase B2 NiAl in all the cases and no other phase is noticed.

3.2.1. Second phase precipitate

Interestingly, the microstructure seen in TEM reveals a second phase precipitate in NiAl matrix (Fig. 4). In spite of the fact that the combustion reactions were carried

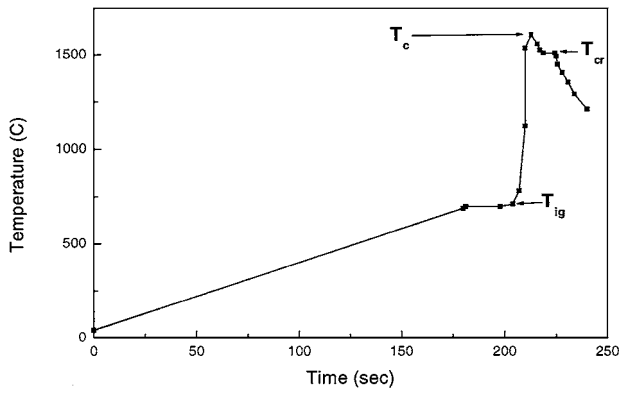

Figure 1 A typical time-temperature profile. T_{ig} is the ignition temperature, T_c is the combustion temperature and T_{cr} is the temperature of crystallization of NiAl.

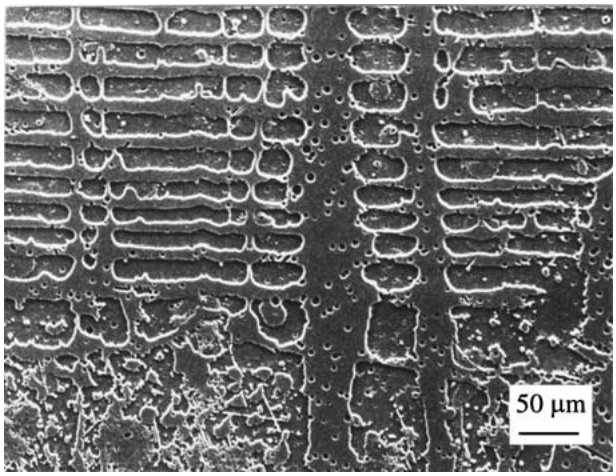

Figure 2 Dendritic microstructure of the product.

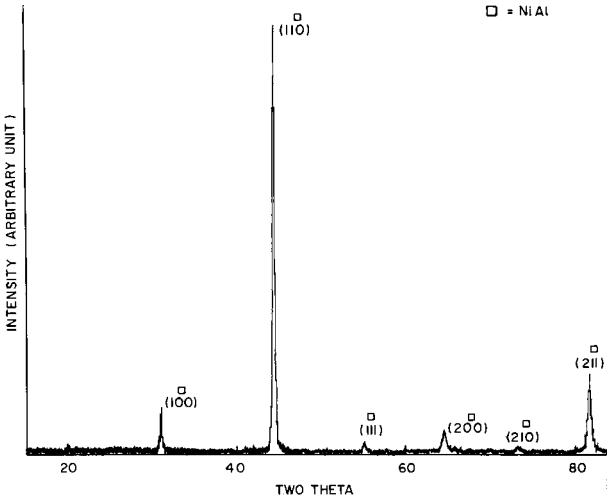

Figure 3 XRD plot showing single-phase NiAl.

out under vacuum or argon atmosphere a very small amount of these precipitates was always noticed. The amount of this phase is found to be below the detection limit of XRD. The precipitates show a variety of shapes that include nearly spherical, cuboidal, ellipsoidal and oblate forms and are found both at the grain boundaries and within the grains. In some cases clusters of precipitates are also observed. Size of the precipitates was measured from the transmission electron micrographs without any stereological correction. They are found to be within a range of 0.33 μm to 1.83 μm. This is a measure of the maximum possible length of the precipitates. One particularly interesting observation is that the size of the initial nickel particles does not show any perceptible influence on the size or the amount of the precipitates. Even though the coarsest nickel powder is approximately 13 times bigger than the finest one, both of them are found to form the second phase precipitates of similar size range and in comparable amount. Results are in essence the same both under the vacuum and in the argon atmosphere. However, though the precipitate occurs in very small quantities; it is worthwhile to characterize these in terms of its chemistry and crystal structure. The details of the analysis have been described elsewhere [15] but a summary of the relevant information is included here.

TABLE II A typical set of EDS data from a precipitate

Element (at.%)	No. of assay				
	1	2	3	4	5
O	71.8	70.5	67.6	71.2	69.3
Al	27.6	29.0	31.7	28.3	30.1
Ni	0.6	0.5	0.7	0.5	0.6

TABLE III Structural details of the precipitate

Point group	Space group	c_H (Å)	a_H (Å)	α-angle (°, 3-layer)	α-angle (°, 6-layer)
$\bar{3}$m	R$\bar{3}$c	12.84	4.855	87	56.65

Chemical analysis reveals that this phase is very rich in oxygen and has only a little nickel in it (Fig. 5). Table II displays a typical dataset of EDS analysis from a single precipitate. A number of such precipitates were analyzed. Fig. 6 shows the corresponding spectra of the B2 NiAl matrix. EPMA analysis of the NiAl matrix was used for the k-factor correction for Ni/Al and the theoretical values of k-factor given by Zaluzec model [16] for O/Al and O/Ni were used. The composition thus corrected is as follows: O : 70.08 at.%, Al : 29.34 at.% and Ni : 0.58 at.%. It does not match with any of the literature-reported values of oxides occurring in this system [17]. Furthermore, the precipitates have shown a remarkable uniformity of chemistry from one to the other irrespective of the nickel particle size.

Crystallographic analysis was carried out to identify this phase using both parallel and convergent beam electron diffraction techniques. This phase was found to have the same crystal structure as α-Al_2O_3 but lattice parameters were different. The results of the analysis are tabulated in Table III. It is recognized to be a solid solution of NiO in Al_2O_3 containing 2.85 mole % NiO. Figs 7 and 8 show the selected area diffraction patterns of some major zone axes from the B2 NiAl matrix and the precipitate phase respectively.

3.3. Result of oxygen analysis

Table IV displays the result of the oxygen analysis of the reactant powders and the products of combustion synthesis. The average oxygen content found in the product is 0.1 wt% or 100 ppm. Ni 3 shows the maximum oxygen content. It is observed that there is little change in the oxygen contents before and after the synthesis reaction. Since, the combustion temperature always exceeded the melting temperature of NiAl, it may be surmised that the oxygen dissociation pressure of the oxide inclusion in the product was much lower than the superincumbent oxygen partial pressure at the NiAl melting point.

TABLE IV Oxygen analysis of the reactant powders and the product

Specimen	Ni 1	Ni 2	Ni 3	Al	Product
Avg. O_2 Content (wt%)	0.1	0.06	0.1	0.1	0.1

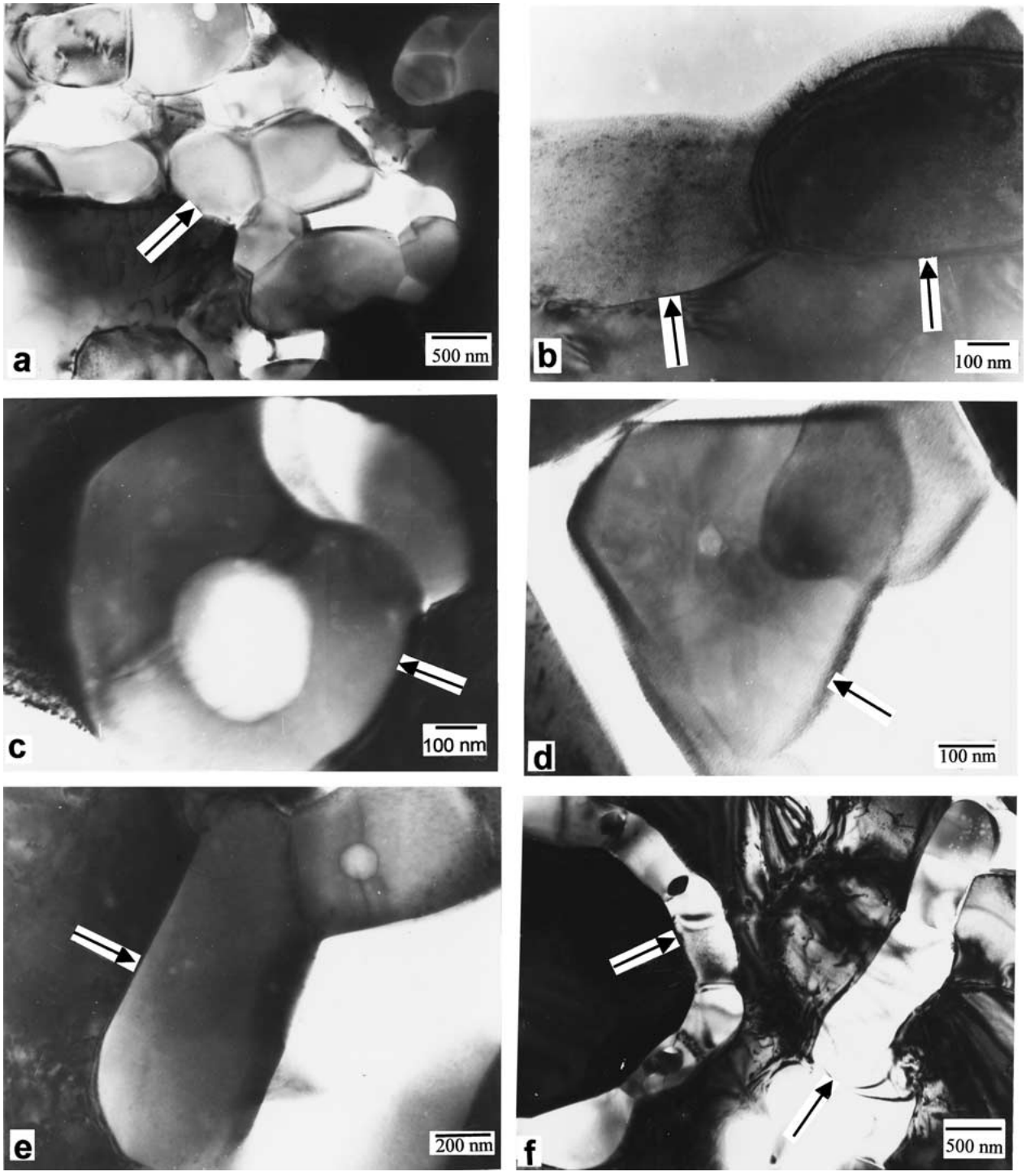

Figure 4 TEM micrograph showing the precipitates.

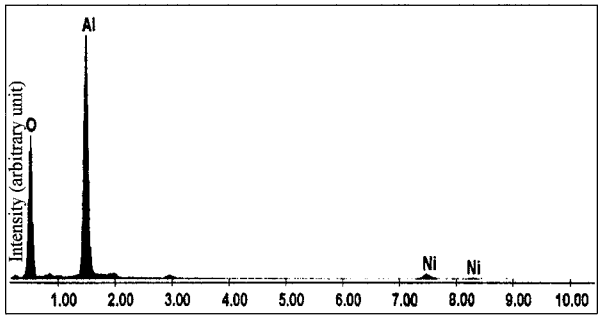

Figure 5 EDS spectra of the precipitate.

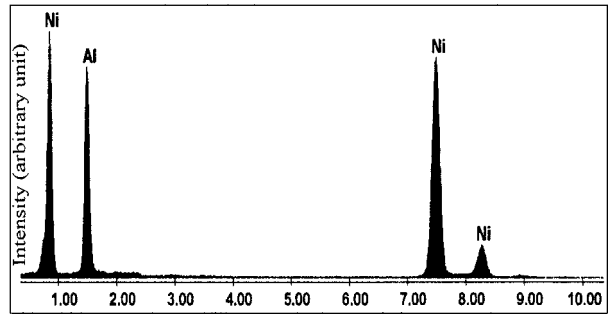

Figure 6 EDS spectra of the matrix.

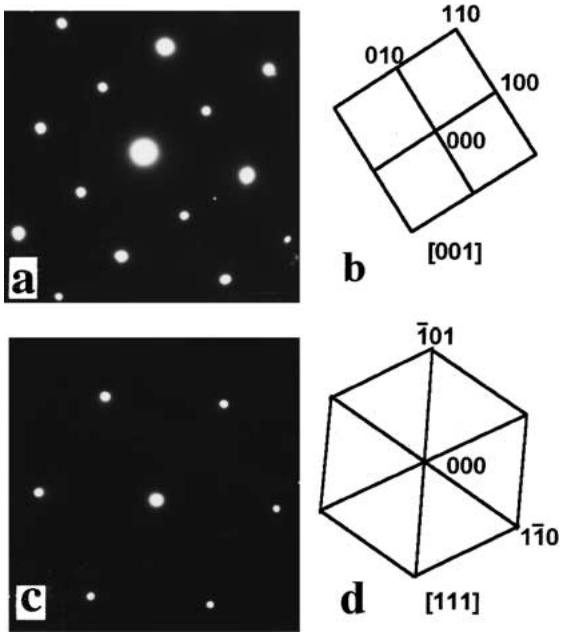

Figure 7 SAD patterns of the matrix and their keys: (a) & (b). [001], (c) & (d). [111].

4. Discussions

The rapid rise of temperature of the specimen, attainment of a very high peak temperature and occurrence of only NiAl phase in the product—all collectively point to the fact that the condensed phase synthesis reaction occurred in the combustion mode. The results further reveal the occurrence of a second phase oxide precipitate in the present case. During SH-synthesis of NiAl this is normally not expected firstly because the process results in rapid rise to a very high temperature when the impurities are expected to volatilize off to give rise to purer products and secondly because the reactions were carried out in pure argon and in vacuum using high purity raw materials. The oxygen that were there in the raw materials and the residual oxygen and moisture in the atmosphere within the reaction chamber are the two possible sources of oxygen for the precipitates. The solubility of oxygen in elemental aluminium is very low. M. Van Lancker [18] reported it to be less than 0.067 at.% in melt and between 0.00025 and 0.0005 at.% in solid state. Solubility of oxygen in solid nickel below the eutectic temperature of 1440°C is also low and is approximately 0.05 at.% [19]. Most of the oxygen normally comes from the particle surface that contains oxide or suboxides of the corresponding metal. Suboxides of aluminium namely, AlO and Al_2O are volatile [9, 20] whereas nickel surfaces are known normally to be covered with NiO which is not volatile [21]. Moreover, aluminium can react with the residual oxygen and moisture present in the atmosphere during the course of the reaction. The results of the thin-film experiments carried out by Prabriputaloong and Piggot [20] in the temperature range of 700°–800°C are extremely relevant in this matter. They performed the experiments in quite similar conditions of vacuum (5×10^{-6} torr) and argon atmosphere. They observed that argon back filling considerably reduced the amounts of oxygen and nitrogen in the reaction chamber but not that of water vapour. Aluminium reportedly reacted with the residual oxygen and water vapour to give rise to Al_2O that remained in the gas phase, according to the following equations:

$$4Al + O_2 = 2Al_2O \quad (1)$$

$$2Al + H_2O = Al_2O + H_2 \quad (2)$$

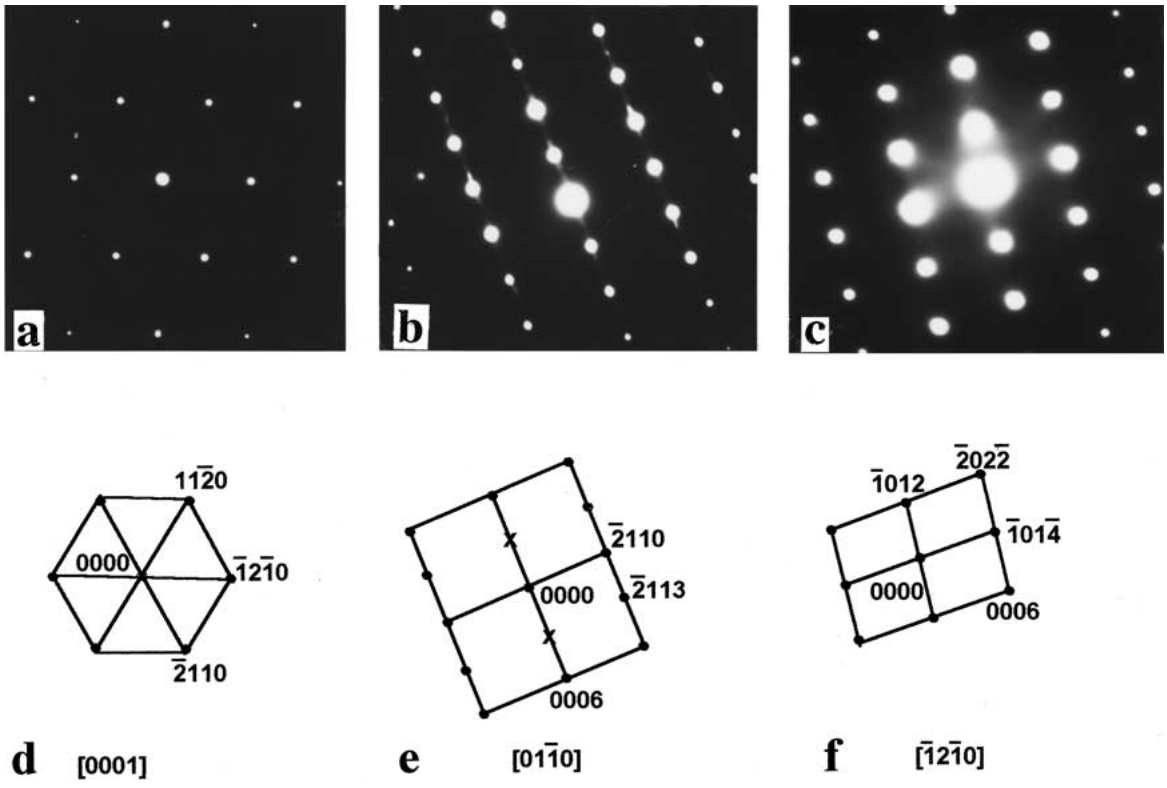

Figure 8 SAD patterns of the precipitate of the following zone axes along with their corresponding keys: (a) & (d). [0001], (b) & (e). [01$\bar{1}$0] (double diffracted reflections are indicated by crosses) and (c) & (f). [$\bar{1}$2$\bar{1}$0].

Both the reactions were found to be thermodynamically feasible even at the very low partial pressures of oxygen and water vapour present in the work. So, similar kind of reactions are very likely to have occurred in the present experiments as well. Nevertheless, a number of different processes must have taken place concurrently. There would be volatilization of both (1). the surface oxides associated with the aluminium particles and (2). the oxygen-deficient one mentioned above that formed during the course of heating up to the ignition point. At the same time, part of the oxygen will remain in solution with molten aluminium since its solubility is more in the melt. On the other hand, the oxide layer present on the surface of nickel particles would get reduced by aluminium giving rise to Al_2O_3. Zhu and Abbaschian [22] showed that this reduction can be both in solid state and liquid state. But, considering the isolated nature of the precipitates the latter seems to be more likely. This reduction reaction can even melt Al_2O_3 since it is highly exothermic [23]. Doty and Abbaschian [24], in fact, utilized this to form alumina-reinforced NiAl composite by reactive hot compaction of a mixture of aluminium and partially oxidized nickel particles. Nevertheless, the amounts of oxygen associated with the nickel particles in the current case are quite low. However, in the case of thermal explosion, the reaction temperature reaches the melting point of the product NiAl within less than one second of reaching the ignition point. So, there can be kinetic restrictions as well to any of the processes mentioned above. The resultant effect is that the second phase may result from (i). the reduction of NiO with or without associated melting and solidification of Al_2O_3 and diffusion of nickel in it; and (ii). the precipitation from molten NiAl during solidification since the solubility of oxygen is more in the melt and very low in the solid state. Interestingly, there has been no significant change in the overall oxygen content on conversion from the reactant to the product.

Moreover, the particle size of the nickel powders does not show any influence on either the size of the precipitates or the total volume percent of the same as indicated earlier. The similar amount of oxygen content in all the three types of nickel particles may be responsible for that. But, the only way nickel particles of sizes differing by approximately thirteen times can have similar amount of oxygen, if the coarse nickel particles are porous agglomerates of fine particles.

The issue of not detecting the presence of the precipitate by XRD can be explained in terms of the low volume fraction of the same. If we assume that the precipitates are spherical and their average diameter is one micron, then 0.1 wt% oxygen corresponds to 0.0053 vol% of precipitate in the product. The density of the precipitate is taken as 4 gm/cc. This volume fraction is well below the detection limit of XRD.

Besides, this study shows experimental evidence of the room temperature solubility of NiO in Al_2O_3 which is not reported in the literature [17]. The only other report about nickel containing alumina was made by Hutchings and Loretto [25]. They observed that oxidation of nickel-rich NiAl (60 at.% Ni) gave rise to an aluminium oxide layer containing approximately 5 at.% nickel, though the figure was only accurate to within a factor of two. More recently, Zalar *et al*. [26] reported about the formation of a thin layer of Al_2O_3 containing a small but unspecified amount of NiO during oxidation of $Ni_{50}Al_{50}$ multilayer.

This study puts forward one more issue which is important from the point of view of the purity of the combustion-synthesized products: Though it has been suggested that combustion synthesis can definitely reduce the impurity levels through removal of volatile and gaseous phases, the possibility of forming oxide precipitates of one or more components cannot be totally ruled out even when the reactions are carried out under vacuum or inert atmosphere, especially in the case of intermetallic synthesis where metallic powders are handled. The formation of an oxide impurity phase and oxygen analysis results suggest that it is difficult to reduce oxygen content in the SH-synthesis of the intermetallics NiAl where a liquid formation starts at low temperature (640°C). This issue of the difficulty involved in achieving self-purification in terms of oxygen impurity was rightly pointed out by Merzhanov [9]. The oxygen content at the particle surface might form oxides or get dissolved in the molten product and precipitate on cooling. So far, it has not been highlighted in the literature possibly because of lack of TEM investigation. Even, in the current system, the presence of the oxide could be traced only by a TEM as it was below the detection limit of XRD.

5. Conclusions

SHS in the thermal explosion mode is a convenient method for synthesis of NiAl. Although SHS is known for removal of impurities and generation of purer products, a small quantity of a second phase precipitate, identified to be a solid solution of NiO in Al_2O_3 was observed in combustion synthesized NiAl. The surface oxygen on the reactant powder particles which is expected to end up evaporating as volatile suboxide under low partial pressure of oxygen, appears to be responsible for its origin. The evidence of the retention of oxygen as sparsely distributed impurity oxide precipitates could be noticed only through TEM. In addition, since the alumina-rich side of the NiO-Al_2O_3 pseudo-binary phase diagram does not show any solubility of NiO in Al_2O_3 at room temperature, further investigation needs to be carried out to resolve the issue.

Acknowledgements

The authors gratefully acknowledge the support received from Dr. S. Banerjee, Associate Director, Materials Group and Head, Materials Science Division. We are thankful to Dr. A. S. Rogachev and Dr. A. Sytschev of Institute of Sructural Macrokinetics and Materials Science, Russia for their help.

References

1. A. G. MERZHANOV, V. M. SHKIRO and I. P. BOROVINSKAYA, 1967, USSR Author's certificate no. 255221, Appl. 1170735, Invent. Bull.

2. A. G. MERZHANOV, in "Combustion and Plasma Synthesis of High-Temperature Materials," edited by Z. A. Munir and J. B. Holt (VCH, Weinheim, 1990) p. 1.
3. Z. A. MUNIR and U. ANSELMI-TAMBURINI, *Mat. Sci. Rep*. **3** (1989) 277.
4. J. J. MOORE and H. J. FENG, *Prog. Mat. Sci.* **39** (1995) 243.
5. A. VARMA, A. S. ROGACHEV, A. S. MUKASYAN and S. HWANG, *Adv. Chem. Engg*. **24** (1998) 79.
6. O. KUBASCHEWSKI, C. B. ALCOCK and P. J. SPENCER, "Materials Thermochemistry," 6th ed. (Pergamon, Elmsford, 1993) p. 299.
7. R. W. CAHN, *Met. Mater. Processes* **1** (1989) 1.
8. N. A. MARTIROSAYN, S. K. DOLUKHANAYN, G. M. MKTRCHAN, I. P. BOROVINSKAYA and A. G. MERZHANOV, *Soviet Powder Metallurgy and Metal Ceramics* **16** (1977) 522.
9. A. G. MERZHANOV, *Comb. Sci. and Tech.* **105** (1995) 295.
10. J. F. CRIDER, *Ceram. Eng. Sci. Proc.* **3** (1982) 519.
11. J. B. HOLT and Z. A. MUNIR, *J. Mater. Sci.* **21** (1986) 251.
12. D. K. CHANG, C. W. WON, B. S. CHUN and G. C. SHIM, *Met. & Mat. Tran. B* **26** (1995) 176.
13. L. J. KECSKES, T. KOTTKE and A. NIILER, *J. Amer. Ceram. Soc.* **73** (1990) 1274.
14. V. N. BLOSHENKO, V. A. BOKII, I. P. BOROVINSKAYA and A. G. MERZHANOV, *Int. J. SHS* **1** (1992) 257.
15. A. BISWAS, K. MADANGOPAL, J. B. SINGH, S. K. ROY and S. BANERJEE, *J. Appl. Cryst.* **33** (2000) 1217.
16. N. J. ZALUZEC, in "Introduction to Analytical Electron Microscopy," edited by J. J. Hren, J. I. Goldstein and D. C. Joy (Plenum, NY, 1979) p. 121.
17. G. PETZOW and G. EFFENBERG (eds.), "Ternary Alloys, A Comprehensive Compendium of Evaluated Constitutional Data and Phase Diagrams," Vol. 7 (VCH, Weinheim, 1993) p. 434.
18. M. VAN LANCKER, "Metallurgy of Aluminium Alloys" (John Wiley & Sons, NY, 1967) p. 40.
19. H. OKAMOTO, P. R. SUBRAMANIAN and L. KACPRZAK (eds.), "Binary Alloy Phase Diagram," Vol. 3, editor-in-chief T. B. Massalski (ASM International, Materials Park, OH, 1990) p. 2831.
20. K. PRABRIPUTALOONG and M. R. PIGGOT, *J. Amer. Ceram. Soc.* **56** (1973) 177.
21. I. I. KORNILOV, "Nickel and its alloys," Vol. I, edited by N. V. Ageev, Translated from Russian, Israel Program for Scientific Translations, Jerusalem (1963) p. 102.
22. H. X. ZHU and R. ABBASCHIAN, *Mat. Sci. & Eng. A* **282** (2000) 1.
23. L. L. WANG, Z. A. MUNIR and Y. M. MAXIMOV, *J. Mater. Sci.* **28** (1993) 3693.
24. H. DOTY and R. ABBASCHIAN, *Mat. Sci. & Eng. A* **195** (1995) 101.
25. R. HUTCHINGS and M. H. LORETTO, *Metal Science* **12** (1978) 503.
26. A. ZALAR, S. HOFMANN, D. KOHL and P. PANJAN, *Thin Solid Films* **270** (1995) 341.

Received 15 January
and accepted 2 November 2001